Molecular dynamics study of the thermodynamics and transport coefficients of hard hyperspheres in six and seven dimensions

L. Lue*
School of Chemical Engineering and Analytical Science, The University of Manchester, P.O. Box 88, Sackville Street, Manchester, M60 1QD, United Kingdom

Marvin Bishop†
Department of Mathematics/Computer Science, Manhattan College, Manhattan College Parkway, Riverdale, New York 10471, USA
(Received 3 April 2006; published 8 August 2006)

Molecular dynamics (MD) simulations are performed for six- and seven-dimensional hard-hypersphere fluids. The equation of state, velocity autocorrelation function, self-diffusion coefficient, shear viscosity, and thermal conductivity are determined as a function of density. The molecular dynamics results for the equation of state are found to be in excellent agreement with values obtained from theoretical approaches and previous MD simulations in seven dimensions. The short-time behavior of the velocity autocorrelation function is well described by the Enskog exponential approximation. The Enskog predictions for the self-diffusion coefficient and the viscosity agree fairly well with the simulation data at low densities, but underestimate these quantities at higher densities. Data for the thermal conductivity are in fine agreement with Enskog theory for all densities and dimensions studied.

DOI: 10.1103/PhysRevE.74.021201 PACS number(s): 51.10+y, 51.20.+d, 64.10.+h, 61.20.Ja

I. INTRODUCTION

It is well known that the structure of fluids is mostly determined by the repulsive portion of the interaction potential between their constituent molecules. Hence, hard spheres offer insight into the behavior of real fluids and provide a good starting point in modeling the thermophysical properties of real fluids. There have been a variety of previous studies of the structure and thermodynamic properties (e.g., equation of state) of hard-hypersphere fluids [1–13] in dimensions higher than 3. Much of this previous work focused on the static and thermodynamic properties of hard-hypersphere fluids. There have been relatively few investigations of the transport properties of these fluids above three dimensions.

A kinetic theory of hard hyperspheres has been developed [14] in the limit of infinite dimensions as a possible reference system for investigating theories in finite dimensions [14–17]. Most of the previous work on transport coefficients in higher dimensions has focused on the self-diffusion coefficient. Michels and Trappeniers [1] obtained the first molecular dynamics results on diffusion in four and five dimensions. Their work was extended by Lue [11] who also computed the shear viscosity and thermal conductivity. Some theoretical analysis of the self-diffusion coefficient was done by Amoros, Maeso, and Villar [18].

In this article, we apply event-driven, equilibrium molecular dynamics (MD) simulations to examine the static and dynamic properties of hard hyperspheres in six and seven dimensions. In addition to the equation of state, we have also investigated the short-time behavior of the velocity autocorrelation function and the transport coefficients such as the self-diffusion coefficient, the shear viscosity, and the thermal conductivity.

*Electronic address: leo.lue@manchester.ac.uk
†Electronic address: marvin.bishop@manhattan.edu

The remainder of this paper is organized as follows. In the following section, the details of the molecular dynamics simulations are given. In Sec. III, the results of the simulation work are presented. Finally, the major findings of this work are summarized in Sec. IV.

II. SIMULATION DETAILS

The algorithm used to perform the MD simulations for the hard hyperspheres is a straightforward generalization to arbitrary dimension d of the standard Alder-Wainwright [19] algorithm for three-dimensional hard spheres. A hypercubic simulation box was employed with periodic boundary conditions. The MD simulations in six dimensions were performed with $N=4096$ hyperspheres whereas the simulations in seven dimensions were done with $N=2187$ or $N=4000$ hyperspheres. For the low-density studies, the systems were started in a hypercubic lattice configuration. For the higher-density simulations the starting configurations were obtained by taking a low-density configuration and performing an MD simulation in which the diameter of the hyperspheres grows linearly with time [20]; once the required density is achieved, this stage of the simulation is halted. For each density, the initial configuration was equilibrated for a duration of 10^6 collisions. Ten separate production runs (trajectories), each consisting of 10^6 collisions, were then performed. The system properties of interest were averaged over these runs, and the statistical errors of the results are reported as one standard deviation from their mean values.

One of the properties that was monitored is t_{avg}, the mean time between collisions for a given particle. For a simulation of N hyperspheres which consists of N_{coll} collisions in a period of time τ, the mean time between collisions is given by $t_{\mathrm{avg}}=\tau N/(2N_{\mathrm{coll}})$. The compressibility factor Z is defined as $Z=\beta P/\rho$ [where $\beta=1/(k_BT)$, k_B is Boltzmann's constant, and T is the absolute temperature], P is the pressure, and ρ is the number density. Z is directly related to t_{avg} by [11]

TABLE I. Six-dimensional results for $N=2000$.

ρ	t_{avg}	D	η	λ
0.5	0.07572±0.00006	0.244±0.003	0.29±0.02	1.6±0.2
0.6	0.05838±0.00006	0.188±0.002	0.39±0.03	2.1±0.3
0.8	0.03754±0.00004	0.121±0.002	0.69±0.06	3.5±0.5
1.0	0.02583±0.00002	0.0797±0.0008	1.11±0.09	6±1
1.2	0.01854±0.00002	0.0513±0.0006	1.9±0.2	9±2
1.4	0.01370±0.00001	0.0314±0.0004	3.4±0.2	13±3
1.6	0.01035±0.00002	0.0170±0.0003	7±1	20±3
1.8	0.00794±0.00002	0.0072±0.0002	15±2	25±7
2.0	0.00612±0.00008	0.0019±0.0002	43±8	40±20

$$Z = 1 + \frac{(\pi\beta m\sigma^2)^{1/2}}{2dt_{avg}}, \tag{1}$$

where m and σ are the hypersphere mass and diameter, respectively.

The transport coefficients D, η, and λ were computed directly from the appropriate Einstein formula [21]. The self-diffusion coefficient is

$$D = \lim_{t\to\infty} \frac{1}{2d}\frac{\partial}{\partial t}\langle[\mathbf{R}_i(t+t_0) - \mathbf{R}_i(t_0)]^2\rangle, \tag{2}$$

where $\mathbf{R}_i(t)$ is the position of particle i at time t and t_0 is the time origin used for averaging. The shear viscosity was computed using the relation [22,23]

$$\eta = \lim_{t\to\infty} \frac{1}{2Vk_BT}\frac{\partial}{\partial t}\langle[W_\eta(t+t_0) - W_\eta(t_0)]^2\rangle, \tag{3}$$

where

$$W_\eta(t+t_0) - W_\eta(t_0) = \sum_{\text{collisions}} \left[\Delta t_c \sum_{k=1}^{N} \dot{x}_k m\dot{y}_k + y_{ij}\Delta m\dot{x}_i\right]. \tag{4}$$

Here, Δt_c is the time between collisions, i and j are the indices of the particles involved in each binary collision, and V is the volume of the simulation box. The thermal conductivity was computed using the relation [22,23]

$$\lambda = \lim_{t\to\infty} \frac{1}{2Vk_BT^2}\frac{\partial}{\partial t}\langle[W_\lambda(t+t_0) - W_\lambda(t_0)]^2\rangle, \tag{5}$$

where

$$W_\lambda(t+t_0) - W_\lambda(t_0) = \sum_{\text{collisions}} \left[\Delta t_c \sum_{k=1}^{N} \dot{x}_k \frac{mv_k^2}{2} + x_{ij}\Delta\frac{mv_i^2}{2}\right]. \tag{6}$$

The values of the various W's were collected at regular time intervals with spacing approximately $t_{avg}/20$. A straight line is fit to the last 80 values of these displacements, and the slope of this fit is used in Eqs. (2), (3), and (5) to determine the transport coefficients.

The normalized velocity autocorrelation function (VAF) as a function of time t, $\psi(t)$, has been computed by averaging over all particles N and all possible velocity origins for the given time displacement, as well as over each of the ten trajectories. Time origins were defined at intervals of roughly $t_{avg}/20$; a total of 100 time intervals were used, which corresponds to a maximum time displacement of roughly $5t_{avg}$.

III. RESULTS AND DISCUSSIONS

Tables I and II present the simulation results for six and seven dimensions, respectively. All quantities are given in reduced hard-hypersphere units (i.e., σ is the unit of length, k_BT is the unit of energy, and m is the unit of mass).

A. Equation of state

Padé fits were developed by Bishop and Whitlock [24] from the high-precision results for the first ten virial coefficients, as reported by Clisby and McCoy [25] and Clisby [26]. In six dimensions, the Padé fit is given by

$$Z_{[4,5]} = \frac{1 + 5.6358\rho + 11.648\rho^2 + 10.539\rho^3 + 3.4170\rho^4}{1 + 3.0520\rho + 1.4857\rho^2 - 0.8228\rho^3 + 0.0694\rho^4 + 0.0154\rho^5} \tag{7}$$

and

$$Z_{[5,4]} = \frac{1 + 5.4689\rho + 10.758\rho^2 + 8.8023\rho^3 + 1.9483\rho^4 - 0.4313\rho^5}{1 + 2.8851\rho + 1.0270\rho^2 - 0.9939\rho^3 + 0.1830\rho^4}, \tag{8}$$

whereas in seven dimensions, it is given by

$$Z_{[4,5]} = \frac{1 + 5.8810\rho + 12.461\rho^2 + 11.291\rho^3 + 3.5776\rho^4}{1 + 3.5187\rho + 2.5736\rho^2 - 0.4615\rho^3 - 0.0638\rho^4 + 0.0261\rho^5} \tag{9}$$

and

TABLE II. Seven-dimensional results for $N=2187$ and 4000.

ρ	N	t_{avg}	D	η	λ
0.6	2187	0.06236±0.00005	0.231±0.004	0.34±0.03	2.1±0.2
0.6	4000	0.06234±0.00007	0.230±0.002	0.33±0.04	1.9±0.4
0.7	2187	0.05063±0.00006	0.187±0.001	0.39±0.02	2.5±0.3
0.8	2187	0.04194±0.00005	0.156±0.002	0.49±0.05	2.9±0.3
0.8	4000	0.04194±0.00004	0.156±0.001	0.51±0.03	3.4±0.4
0.9	2187	0.03537±0.00003	0.131±0.002	0.62±0.04	3.5±0.4
1.0	4000	0.03023±0.00004	0.1113±0.0009	0.78±0.08	4.4±0.9
1.1	4000	0.02610±0.00003	0.0950±0.0008	0.93±0.06	6±1
1.2	4000	0.02274±0.00002	0.0812±0.0006	1.1±0.1	7±1
1.3	4000	0.01996±0.00001	0.0698±0.0005	1.4±0.2	7.5±0.9
1.4	4000	0.01763±0.00002	0.0598±0.0004	1.7±0.1	9±2
1.5	4000	0.01567±0.00002	0.0511±0.0006	2.1±0.2	11±1
1.6	4000	0.01398±0.00002	0.0434±0.0003	2.5±0.2	13±2
1.7	4000	0.01254±0.00001	0.0365±0.0004	3.0±0.2	16±3
1.8	4000	0.01128±0.00001	0.0307±0.0003	3.8±0.3	16±2

$$Z_{[5,4]} = \frac{1 + 4.6594\rho + 5.8738\rho^2 - 1.3949\rho^3 - 6.6540\rho^4 - 2.7188\rho^5}{1 + 2.2970\rho - 1.1277\rho^2 - 2.4788\rho^3 + 0.4591\rho^4}. \tag{10}$$

The simulation results for the variation of the compressibility factor with density are presented in Fig. 1. In six and seven dimensions, the simulation data are well described by both the [4,5] and [5,4] Padé approximants. In seven dimensions, our MD data for the equation of state are also in excellent agreement with the MD data of Robles, de Haro, and Santos [10], who used systems of 64 particles.

B. Velocity autocorrelation function

Figure 2 presents the VAF's for six-dimensional hard-hypersphere fluids for all nine densities studied ($\rho = 0.5-2.0$). The density decreases going from left to right. A negative backscattering region is apparent at densities higher than about 1.0. Bishop, Michels, and de Schepper [27] extended the Enskog theory developed by de Schepper, Ernst, and Cohen [28], which related the value of the self-diffusion coefficient D_E to t_{avg}, to obtain an expression for D_E:

$$D_E = \frac{\pi^{1/2}}{4(Z-1)} = \frac{dt_{avg}}{2} = t_E, \tag{11}$$

where t_E is the Enskog time scale. Bishop and co-workers [27] have previously studied the short-time behavior of the

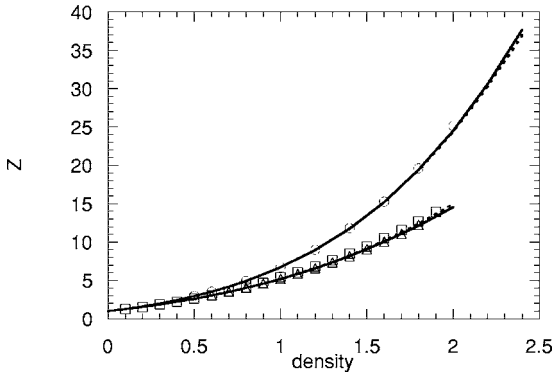

FIG. 1. Equation of state of hard-hypersphere fluids in six and seven dimensions. The symbols are the results of MD simulations. The circles are from the present work for $d=6$, and the triangles are from the present work for $d=7$. The squares are for MD simulation from Ref. [10] for $d=7$. The solid lines are the $Z_{[4,5]}$ Padé approximants, and dotted lines are the $Z_{[5,4]}$ Padé approximants.

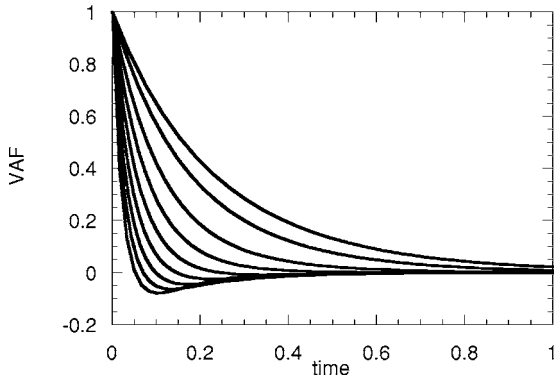

FIG. 2. The velocity autocorrelation function for $d=6$ as a function of time for $\rho=0.5$, 0.6, 0.8, 1.0, 1.2, 1.4, 1.6, 1.8, and 2.0 (from right to left).

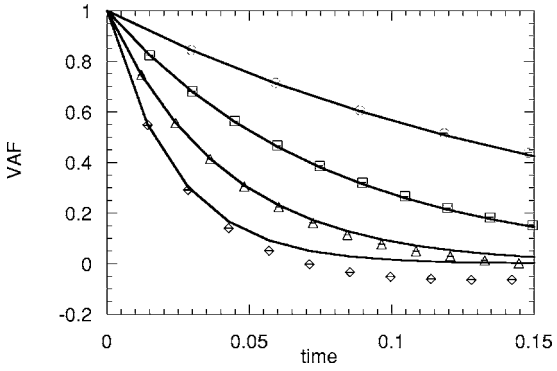

FIG. 3. The short-time behavior of the velocity autocorrelation function for $d=6$: $\rho=0.6$ (circles), $\rho=1.0$ (squares), $\rho=1.4$ (triangles), and $\rho=1.8$ (diamonds). The lines are the Enskog predictions of Eq. (12).

VAF of hard hyperspheres in three, four, and five dimensions and showed that the short-time dependence of the VAF, $\psi(t)$, varied with time as

$$\psi(t) \approx e^{-t/D_E}. \tag{12}$$

This exponential decay is a consequence of assuming that all the collisions are uncorrelated. Deviations from this expression are due to the correlations between collisions, caused by multiple collisions and backscattering, which become more likely as the density increases.

In Fig. 3, the short-time behavior of a selection of the VAF's is presented with densities ranging from 0.6 to 1.8 in steps of 0.4. Note that the uncertainties in the simulation values are smaller than the plotting symbols. From this figure it is clear that the Enskog approximation is good at short times even for the highest-density states.

In seven dimensions, 13 densities ($\rho=0.6-1.80$) were investigated. Two states ($\rho=0.6$ and 0.8) were studied with both 2187 and 4000 particles. The corresponding VAF's for the two states with differing numbers of particles are identical within statistical scatter. Figure 4 presents the VAF's for seven dimensions. The 2187-particle results are indicated with dashed lines. As was the case in six dimensions, the

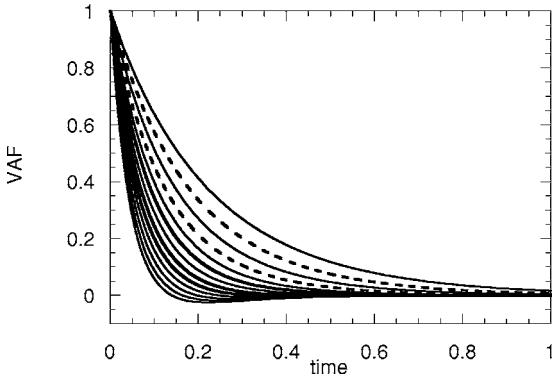

FIG. 4. The velocity autocorrelation function for $d=7$ as a function of time $\rho=0.6$, 0.7, 0.8, 0.9, 1.0, 1.1, 1.2, 1.3, 1.4, 1.5, 1.6, 1.7, and 1.8 (from right to left). The dashed lines at $\rho=0.7$ and 0.9 are for $N=2187$, whereas all the other states are for $N=4000$.

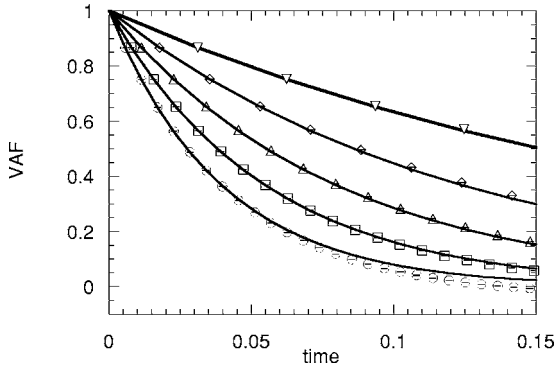

FIG. 5. The short-time behavior of the velocity autocorrelation function for $d=7$: $\rho=0.6$ (downward triangles), $\rho=0.9$ with $N=2187$ (diamonds), $\rho=1.2$ (upward triangles), $\rho=1.5$ (squares), and $\rho=1.8$ (circles). The lines are the predictions of Enskog theory [see Eq. (12)].

data are very smooth. The density decreases as one goes from left to right. For this system, the negative backscattering region is present at densities greater than about 1.4.

Figure 5 presents the short-time behavior of the VAF's for a range of densities from 0.6 to 1.8. Note that the data for $\rho=0.9$ are for $N=2187$, while the rest of the data are for $N=4000$. As was found in six dimensions, there is very good agreement at short times for all the densities examined. The error bars are again smaller than the plotting symbols. Note that the fit to theory is even better in seven dimensions than in six dimensions because at the same reduced densities caging is less likely in the higher-dimensional system.

C. Transport coefficients

Figure 6 compares the self-diffusion coefficient D from MD simulations to the value predicted by the Enskog theory, D_E. Our results in six and seven dimensions are similar to those found by Lue [11] and Amoros, Maeso, and Villar [18] in three, four, and five dimensions. Enskog theory slightly underpredicts the value of the self-diffusion coefficient (i.e.,

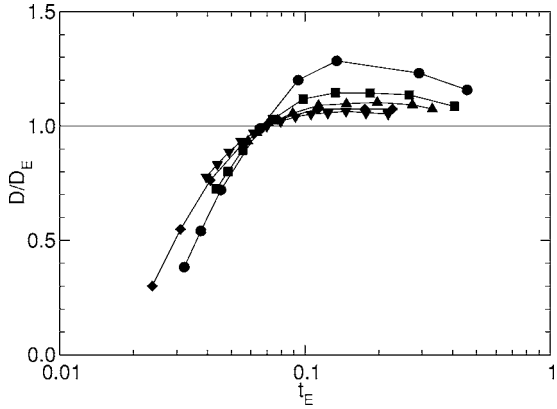

FIG. 6. Variation of the self-diffusion coefficient for $d=3$ (circles, Ref. [11]), $d=4$ (squares, Ref. [11]), $d=5$ (upward triangles, Ref. [11]), $d=6$ (diamonds, this work), and $d=7$ (downward triangles, this work) dimensions as a function of the Enskog time.

D/D_E is slightly greater than 1.0) at larger Enskog times ($t_E > 0.07$) but significantly overpredicts the value at shorter Enskog times ($t_E < 0.07$). Larger Enskog times correspond to lower densities since the average time between collisions will increase as the density is decreased. Moreover, there is a dimensional effect. Enskog theory becomes uniformly better (i.e., D/D_E becomes closer to 1.0), at both low and high Enskog times, as the dimension of the fluid increases. At higher dimensions, the recollision contributions to the dynamics are less significant. At lower values of t_E, which correspond to higher densities, the deviations from the Enskog predictions are extremely large and increase as the density increases. However, it is interesting to note that the point at which Enskog theory crosses over from overpredicting to underpredicting D seems to be relatively independent of the dimensionality of the system.

With decreasing density, the transport coefficients of fluids approach the Boltzmann limit. For hard-hypersphere fluids, the Boltzmann expression for the viscosity, η_B, in hard-hypersphere units, is given by [29–31]

$$\eta_B = \frac{\pi^{1/2}(d+2)}{8dB_2}, \tag{13}$$

where B_2 is the second virial coefficient of a d-dimensional hypersphere:

$$B_2 = \frac{\pi^{d/2}\sigma^d}{d\Gamma(d/2)}. \tag{14}$$

Here, Γ is the standard Gamma function. The Boltzmann expression for the thermal conductivity λ_B is given by

$$\lambda_B = \frac{\pi^{1/2}(d+2)^2}{16B_2(d-1)}. \tag{15}$$

Lutsko [31] recently obtained the transport coefficients of dissipative (nonelastic) hard-sphere fluids using Enskog theory within the lowest-order Sonine approximation. His Enskog expression for the viscosity η_E in the elastic limit [$\alpha=1$ in Eq. (99) Ref. [31]] is given by

$$\frac{\eta_E}{\eta_B} = \frac{1}{\chi} + \frac{4B_2\rho}{d+2} + 4\chi\left(1+\frac{4d}{\pi}\right)\left(\frac{B_2\rho}{d+2}\right)^2, \tag{16}$$

and for the thermal conductivity λ_E is given by

$$\frac{\lambda_E}{\lambda_B} = \frac{1}{\chi} + \frac{6B_2\rho}{d+2} + 4\chi\left[\frac{9}{4}+\frac{4(d-1)}{\pi}\right]\left(\frac{B_2\rho}{d+2}\right)^2, \tag{17}$$

where χ is the contact value of the pair correlation function [i.e., $g(\sigma^+)$]. Note that χ can be directly obtained [13] from the compressibility factor Z:

$$\chi = \frac{(Z-1)}{B_2\rho}. \tag{18}$$

Combining Eqs. (1) and (18), χ can also be related directly to the mean time between collisions:

$$\chi = \frac{\pi^{1/2}}{2dB_2\rho t_{\text{avg}}}. \tag{19}$$

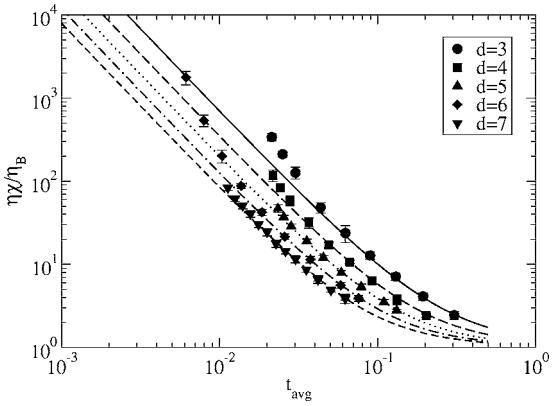

FIG. 7. Log-log plot of the variation of the viscosity with t_{avg} for hard-hyperspherical fluids in dimensions 3–7. Symbols are from molecular dynamics simulations, and the curves are the predictions of Enskog theory [Eq. (16)]: $d=3$, circles and solid line; $d=4$, squares and long-dashed line; $d=5$, upward-triangles and dotted line; $d=6$, diamonds and dashed-dotted line; $d=7$, downward-triangles and short-dashed lines.

The three distinct terms in Eqs. (16) and (17) represent the contributions of the kinetic term, the kinetic-potential cross term, and the potential term in the transport coefficients [32,33]. These equations extend previous results in two and three dimensions.

In two dimensions, Gass [34] found a coefficient of 0.8729 compared to the prediction of 0.8866 for the shear viscosity [Eq. (16)] and a value of 0.8729 compared to the predicted 0.8808 for the thermal conductivity [Eq. (17)]. In three dimensions, the calculations of Résibois and de Leener [35] for the shear viscosity and thermal conductivity in three dimensions agree exactly with Eqs. (16) and (17), respectively. The higher-order third Sonine polynomial approximation leads [32,33] to a coefficient value of 0.761 compared to Lutsko's prediction of 0.771 for the shear viscosity and a value of 0.755 compared to the predicted 0.767 for the thermal conductivity.

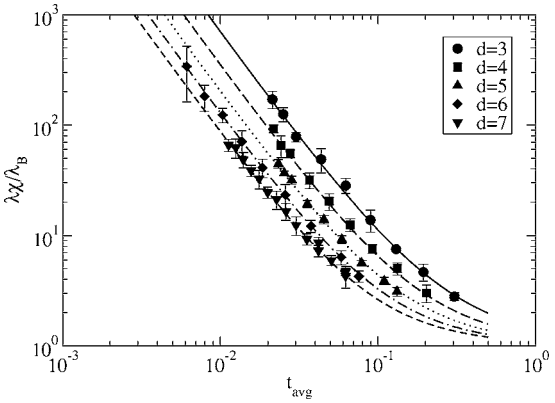

FIG. 8. Log-log plot of the variation of the thermal conductivity with t_{avg} for hard-hyperspherical fluids in dimensions 3–7. Symbols are from molecular dynamics simulations and the curves are the predictions of Enskog theory [Eq. (17)]: $d=3$, circles and solid line; $d=4$, squares and long-dashed line; $d=5$, upward-triangles and dotted line; $d=6$, diamonds and dashed-dotted line; $d=7$, downward-triangles and short-dashed lines.

The variation of the viscosity of hard hyperspheres with the average time between collisions is shown in Fig. 7. The symbols indicate our MD simulation data (with error bars) and the lines are the d-dimensional Enskog theory [Eq. (16)]. The MD data of Lue [11] and the corresponding Enskog predictions for three, four, and five dimensions are also shown. It is clearly seen that the simulation and theory are in excellent agreement at low and moderate densities (large collision times) and that the agreement improves as the dimension of the system increases.

A similar plot is presented for the thermal conductivities in Fig. 8. Again excellent agreement is obtained at low and moderate densities and the agreement improves as the dimension increases. In fact, the MD thermal conductivity data agree even more closely with the d-dimensional Enskog theory than was found for the shear viscosity. To explain this result one needs to consider the underlying mechanisms responsible for shear viscosity and thermal conductivity. Viscosity requires momentum transport whereas thermal conductivity needs energy transport. As the density increases (t_{avg} decreases) it becomes more difficult for particles to move but energy exchange is less restricted than momentum exchange. At higher dimensions these effects are less severe and they will occur at higher densities.

IV. CONCLUSIONS

Molecular dynamics simulations were performed for six- and seven-dimensional hard-hypersphere fluids. The equation of state is in excellent agreement with data from other workers. We have also obtained very good agreement with the Enskog predictions for the short-time behavior of the velocity autocorrelation function in six and seven dimensions, as well as fine agreement with the d-dimensional Enskog predictions for the shear viscosity and thermal conductivity. We plan to extend our calculations to higher densities in order to investigate the properties of the crystalline phases.

ACKNOWLEDGMENTS

This research has been supported by the Manhattan College Computer Centers. We wish to thank Paula Whitlock for helpful comments on the manuscript and Nikolai Brilliantov and Andres Santos for pointing us to Ref. [31].

[1] J. P. J. Michels and N. J. Trappeniers, Phys. Lett. **104A**, 425 (1984).
[2] M. Baus and J. L. Colot, Phys. Rev. A **36**, 3912 (1987).
[3] J. Amoros, J. R. Solana, and E. Villar, Phys. Chem. Liq. **19**, 119 (1989).
[4] J. Amoros and E. Villar, Phys. Chem. Liq. **21**, 51 (1990).
[5] D. J. Gonzalez, L. E. Gonzalez, and M. Silbert, Phys. Chem. Liq. **22**, 95 (1990).
[6] M. Luban and J. P. J. Michels, Phys. Rev. A **41**, 6796 (1990).
[7] M. Bishop, A. Masters, and J. H. R. Clarke, J. Chem. Phys. **110**, 11449 (1999).
[8] A. Santos, J. Chem. Phys. **112**, 10680 (2000).
[9] M. Gonzalez-Melchor, J. Alejandre, and M. Lopez de Haro, J. Chem. Phys. **114**, 4905 (2001).
[10] M. Robles, M. L. de Haro, and A. Santos, J. Chem. Phys. **120**, 9113 (2004).
[11] L. Lue, J. Chem. Phys. **122**, 044513 (2005).
[12] M. Bishop, P. A. Whitlock, and D. Klein, J. Chem. Phys. **122**, 074508 (2005).
[13] M. Bishop and P. A. Whitlock, J. Chem. Phys. **123**, 014507 (2005).
[14] Y. Elskens and H. L. Frisch, Phys. Rev. A **37**, 4351 (1988).
[15] H. L. Frisch, N. Rivier, and D. Wyler, Phys. Rev. Lett. **54**, 2061 (1985).
[16] B. Bagchi and S. A. Rice, J. Chem. Phys. **88**, 1177 (1988).
[17] H. L. Frisch and J. K. Percus, Phys. Rev. E **60**, 2942 (1999).
[18] J. Amoros, M. J. Maeso, and E. Villar, Phys. Chem. Liq. **24**, 55 (1991).
[19] B. J. Alder and T. E. Wainwright, J. Chem. Phys. **31**, 459 (1959).
[20] L. Lue and L. V. Woodcock, Int. J. Thermophys. **23**, 937 (2002).
[21] E. Helfand, Phys. Rev. **119**, 1 (1960).
[22] B. J. Alder, D. M. Gass, and T. E. Wainwright, J. Chem. Phys. **53**, 3813 (1970).
[23] S. W. Smith, C. K. Hall, and B. D. Freeman, J. Chem. Phys. **102**, 1057 (1995).
[24] M. Bishop and P. A. Whitlock (private communication).
[25] N. Clisby and B. M. McCoy, J. Stat. Phys. **122**, 15 (2006).
[26] N. Clisby, Ph.D. thesis, SUNY, Stony Brook (2004).
[27] M. Bishop, J. P. J. Michels, and I. M. de Schepper, Phys. Lett. **111A**, 169 (1985).
[28] I. M. de Schepper, M. H. Ernst, and E. G. D. Cohen, J. Stat. Phys. **25**, 321 (1981).
[29] J. J. Brey and D. Cubero, *Granular Gases* (Springer-Verlag, Berlin, 2001).
[30] J. J. Brey and M. J. Ruiz-Montero, Phys. Rev. E **70**, 051301 (2004).
[31] J. F. Lutsko, Phys. Rev. E **72**, 021306 (2005).
[32] J. O. Hirschfelder, C. F. Curtis, and R. B. Bird, *Molecular Theory of Gases and Liquids* (Wiley, New York, 1954).
[33] S. Chapman and T. G. Cowling, *The Mathematical Theory of Non-Uniform Gases* (Cambridge University Press, Cambridge, England, 1960).
[34] D. Gass, J. Chem. Phys. **54**, 1898 (1971).
[35] P. Résibois and M. de Leener, *Classical Kinetic Theory of Fluids* (Wiley, New York, 1977).